of metallic W ($\rho = 19.32$ g cm^{-3}). The HRTEM investigation showed that this structure is rather stable under atmospheric pressure and electron-beam irradiation.

The results of this work demonstrate the high power of HRTEM in structure analysis of very small crystal fragments. Small differences between experimental and theoretical images can be explained by some vagueness of imaging parameters (Δf, C_s, *etc.*).

The procedure of image processing used in this paper is similar to that proposed by Hovmöller, Sjogren, Farrauts, Sundberg & Marinder (1984). However, there are some differences connected with phase-origin determination [equation (1)] and the linear transformation of the selected image area to have integer unit-cell numbers in the frame memory 256 × 256 pixels. We used the structure refinement procedure [equation (3)] and this made it possible to minimize the differences between experimental and theoretical images and to determine the cation positions more accurately. It was found that the effectiveness of this procedure improves as the number of reflections used for image formation increases.

It is a pleasure to thank Drs E. V. Orlova and M. B. Sherman for their skillful assistance and cooperation in image processing.

References

HÄGG, G. Z. (1935). *Z. Phys. Chem. Abt. B*, **29**, 192–196.
HARTMANN, H., EBERT, F. & BRETSCHNEIDE, O. (1931). *Z. Anorg. Chem.* **198**, 127–132.
HOVMÖLLER, S., SJOGREN, A., FARRAUTS, G., SUNDBERG, M. & MARINDER, B.-O. (1984). *Nature (London)*, **311**, 238–241.
MAGNÉLI, A. (1949). *Ark. Kemi*, **1**, 223–227.
MAGNÉLI, A. (1950). *Ark. Kemi*, **1**, 513–518.
MAGNÉLI, A. & ANDERSSON, S. (1955). *Acta Chem. Scand.* **9**, 1378–1381.
PALMER, D. J. & DICKENS, P. G. (1979). *Acta Cryst.* B**35**, 2199–2201.
ROTH, R. S. & WADSLEY, A. D. (1965). *Acta Cryst.* **19**, 26–32, 32–38, 38–42, 42–47.
ROTH, R. S. & WARING, J. L. (1966). *J. Res. Natl Bur. Stand. Sect. A*, **70**, 281–303.
SUNDBERG, M. (1978). *Chem. Scr.* **14**, 161–166.
ZAKHAROV, N. D., GRIBELUK, M. A., VAINSHTEIN, B. K., KOVBA, L. M. & HORIUCHI, S. (1988). *Acta Cryst.* A**44**, 821–827.
ZAKHAROV, N. D., GRIBELUK, M. A., VAINSHTEIN, B. K., ROZANOVA, O. N., UCHIDA, K. & HORIUCHI, S. (1983). *Acta Cryst.* B**39**, 575–579.

Acta Cryst. (1992). B**48**, 577–584

X-ray Standing-Wave Analysis of the Bi Preferential Distribution in $Y_{3-x}Bi_xFe_5O_{12}$ Thin Films

BY A. YU. KAZIMIROV, M. V. KOVALCHUK AND A. N. SOSPHENOV

A. V. Shubnikov Institute of Crystallography of the Academy of Sciences of Russia, Leninsky pr. 59, *Moscow* 117333, *Russia*

V. G. KOHN

I. V. Kurchatov Institute of Atomic Energy, Kurchatov Square 46, *Moscow* 123182, *Russia*

J. KUB, P. NOVÁK AND M. NEVŘIVA

Institute of Physics of the Czechoslovak Academy of Sciences, Cukrovarnicka 10, 16200 *Prague* 6, *Czechoslovakia*

AND J. ČERMÁK

Czech Technical University, Suchbatarova 4, 16607 *Prague* 6, *Czechoslovakia*

(*Received* 28 *January* 1991; *accepted* 10 *February* 1992)

Abstract

The X-ray standing-wave method was used to study the distribution of bismuth ions on the dodecahedral sublattice of a thin yttrium–bismuth iron garnet film. The film was grown epitaxially on a (001)-oriented substrate of gadolinium gallium garnet. Measurement of the fluorescence of Bi^{3+}, Y^{3+}, Fe^{3+} and Gd^{3+} ions was made under conditions such that an X-ray standing wave was formed during diffraction from the layer studied. We have shown experimentally that the dodecahedral sites c_z and c_{xy} are not

0108-7681/92/050577-08$06.00

equivalent – the fraction of Bi^{3+} ions in c_z positions is 0.44 ± 0.02 and in c_{xy} positions 0.56 ± 0.02, while in the case of crystallographically equivalent sites (or, for a uniform distribution of Bi^{3+} ions over dodecahedral sites) these fractions are $\frac{1}{3}$ and $\frac{2}{3}$, respectively.

1. Introduction

Epitaxial thin films of ferrimagnetic garnets containing bismuth are promising materials for various magnetooptical and bubble applications (Hansen & Krumme, 1984). One of the essential properties, which must be optimized with respect to the specific application, is growth-induced magnetic anisotropy. A necessary condition for this to occur is a preferential non-cubic distribution of Bi^{3+} ions on the dodecahedral sublattice of the garnet. This preferential distribution arises during growth and depends on a number of factors such as substrate orientation, film composition and growth conditions (melt composition, supercooling *etc.*).

It is generally accepted (Winkler, 1981; Hansen & Krumme, 1984) that the reason for this preferential distribution is the different binding energies of the Bi^{3+} ions on the crystal surface at different dodecahedral sites (the sites differ in terms of the orientation of the local coordinate system with respect to the growth direction). It is not feasible to estimate the extent of the preferential distribution theoretically and until now no direct experimental method by which to determine it existed. Note that once the preferential distribution is known, the single ion model for the anisotropy may be used to analyze the growth-induced anisotropy (Novak, 1984).

Let us briefly summarize the principles of the X-ray standing-wave (XSW) method. During dynamical Bragg diffraction an XSW arises with a wavelength equal to the distance between the diffracting planes (Batterman & Cole, 1964; Pinsker, 1978). The change in angle of incidence of the X-rays within the region of total reflection leads to a shift of the standing wave by one half wavelength, which in turn leads to a change in the yield of various secondary radiation sources (*e.g.* fluorescence). This yield is determined by the positions of the atoms in the elementary cell relative to the nodes and antinodes of the XSW (Batterman, 1964). Measurement of the fluorescence then leads to the possibility of localizing the fluorescent atoms relative to the diffracting planes (Batterman, 1969). During the last few years this method has been used successfully in localizing impurity atoms and atoms absorbed on the surface of crystals (for a survey see Kovalchuk & Kohn, 1986). For compound crystals the XSW method allows the structure of individual sublattices to be studied. The sensitivity of fluorescence yield to the crystallographic position of ions in crystals with the garnet structure was demonstrated by Lagomarsino, Scarinci & Tucciarone (1984).

Until recently, localization of atoms by the XSW method meant that the standing wave had to be generated in the lattice of a perfect or nearly perfect crystal. Kazimirov, Kovalchuk & Kohn (1988) studied the behaviour of the XSW in a thin heteroepitaxial film during the diffraction of X-rays by the investigated layer itself. The sensitivity of the fluorescence yield to the crystallographic positions of the atoms in the heteroepitaxial film unit cell was demonstrated. Fluorescence from epitaxial films of yttrium iron garnet was studied by Zheludeva, Zakharov, Kovalchuk, Kohn, Sozontov & Sosfenov (1988). So, the excitation of the XSW in the investigated layer itself opens up the possibility of studying the structure of thin films with compound composition which cannot be obtained as perfect bulk crystals.

In the present paper the XSW method is used to study the positions of Bi^{3+} ions in the lattice of a heteroepitaxial film of yttrium–bismuth iron garnet. The main task is to determine quantitatively the distribution of bismuth over the different dodecahedral positions which are occupied by yttrium in a pure yttrium iron garnet. This task is solved by detailed analysis of the angular dependence of the Bi^{3+} fluorescence. In addition, the fluorescence yield of Y^{3+} and Fe^{3+} ions from the film and Gd^{3+} ions from the substrate and X-ray diffraction curves were measured and analysed. All of the experimental results obtained are well described by the theory.

In the next section the structural details of the system studied and the selection of the diffracting planes are discussed. In §3 we give a brief account of the theoretical basis of the XSW method and the results of our calculations. The experimental setup and the methods used are described in §4. In §5 the experimental results are presented and discussed.

2. Noncubic distribution of ions in garnet

Ideal garnets have cubic symmetry with cations entering octahedral (*a*), tetrahedral (*d*) and dodecahedral (*c*) sublattices. In the $Y_{3-x}Bi_xFe_5O_{12}$ system Bi^{3+} and Y^{3+} ions only enter the *c* sites, while *a* and *d* sublattices are fully occupied by the Fe^{3+} ions (Winkler, 1981). There are 16 *a*, 24 *d* and 24 *c* sites in the elementary cell. The local symmetry of *a* and *d* sites is axial, while the symmetry of *c* sites is rhombic. In the ideal infinite garnet lattice all sites belonging to the same sublattice are equivalent – they are related by the symmetry operations of the cubic O_h^{10} group of the garnet structure. For sites on the surface of a thin garnet film such complete equivalency no longer exists, only the sites which are

related by rotation around the growth direction remain equivalent. As far as the distribution of ions between the sites is concerned, the equivalency also holds for sites related by inversion.

For the [001] growth direction there are two inequivalent groups of dodecahedral sites, the first consists of 16 sites which are denoted as c_{xy}, the second consists of 8 sites denoted as c_z [see Novak (1984) for a more thorough discussion]. The distribution of c_{xy} and c_z sites within the elementary cell for this growth direction is shown in Fig. 1. Note that the sites belonging to the c_{xy} and c_z groups lie in different layers and consequently they may be distinguished by the XSW method.

3. Theory

It is known (Kazimirov, Kovalchuk & Kohn, 1988) that if the yield depth of fluorescence radiation L_{yi} is much smaller than the extinction length L_{ex}, the angular dependence of the intensity of fluorescence radiation under the diffraction of σ-polarized X-rays in a compound crystal is given by

$$\kappa^{\nu}(\Delta\theta) \simeq |E_o|^2 + |E_h|^2 + 2|E_o E_h| f_c^{\nu} \cos[\alpha(\Delta\theta) + \varphi_h^{\nu}] \quad (1)$$

where E_o, E_h are the amplitudes of the incident and diffracted waves, $f_c^{\nu} = |S_h^{\nu}| \exp(-M_h^{\nu} - W_h^{\nu})$, and $|S_h^{\nu}|$ and φ_h^{ν} are the amplitude and phase of the structure factor of the crystal sublattice which is occupied by ions of the type ν. $S_h^{\nu} = \sum_k \exp(-i\mathbf{h}\boldsymbol{\rho}_k^{\nu})$, N_{ν} is the total number and $\boldsymbol{\rho}_k^{\nu}$ the positions of ν ions in the elementary cell. $\exp(-W_h^{\nu})$ is the static Debye–Waller factor describing the random displacements of ions from their equilibrium positions in a perfect lattice. $\alpha(\Delta\theta)$ is the phase of the complex ratio E_h/E_o. In the angular region of total reflection the phase $\alpha(\Delta\theta)$ changes from 0 to π which in turn moves the nodes and antinodes of the XSW by half a wavelength.

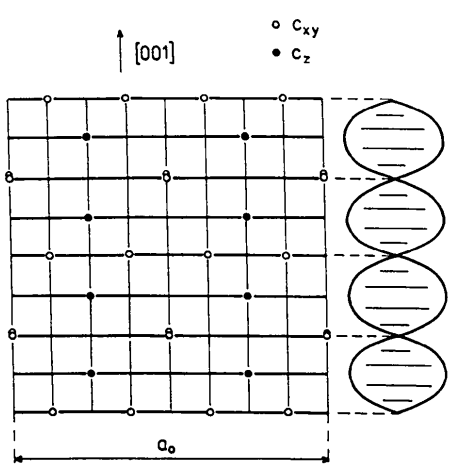

Fig. 1. Projection of the dodecahedral positions c_z (full circles) and c_{xy} (open circles) on the plane (001). The (004) X-ray standing wave is also shown schematically.

According to (1) the fluorescence yield angular curve for certain groups of atoms is determined by the structure factor of the sublattice of these atoms (note the importance of phase here). At the same time the reflection coefficient $|E_h|^2/|E_o|^2$ is determined only by the modulus of the structure factor of the elementary cell as a whole and gives no direct information about the phase. This feature opens up the unique possibilities of the XSW method *i.e.* the structure analysis of compound crystals by the measurement of fluorescence radiation.

Let us now discuss the structure factors of the different cation sublattices in the garnet structure for the (004) reflection. For octahedral (a), tetrahedral (d) and dodecahedral (c) sublattices we have: $S_h^a = 1$ (16 sites in the elementary cell), $S_h^d = \frac{1}{3}$ (24 sites) and $S_h^c = \frac{1}{3}$ (24 sites). So, the structure factors of gadolinium (c sites) and gallium (a and d sites) ions in the gadolinium gallium garnet crystal are $S_h^{Gd} = \frac{1}{3}$ and $S_h^{Ga} = 0.6$.

As discussed in §2, c sites in the (001)-oriented films are not equivalent. For the reflection (004) the inequivalent groups of sites c_z and c_{xy} have different structure factors $S_h(c_z) = -1$ (8 sites), $S_h(c_{xy}) = +1$ (16 sites). The structure factor of the Bi^{3+} ions, which enter the dodecahedral sublattice in $Y_{3-x}Bi_x$-Fe_5O_{12} garnet films, is influenced by the distribution of these ions between c_z and c_{xy} positions. We denote by p the fraction of Bi^{3+} ions in c_z positions:

$$p = N_z^{Bi}/(N_z^{Bi} + N_{xy}^{Bi}),$$

where N_z^{Bi}, N_{xy}^{Bi} are the numbers of Bi^{3+} ions in c_z and c_{xy} sites, respectively. Then the structure factor of Bi^{3+} ions for the (004) reflection is $S_h^{Bi} = 1 - 2p$. The uniform distribution of Bi^{3+} ions between c_z and c_{xy} sites corresponds to $p = \frac{1}{3}$. We emphasize that the main task of the present work is the experimental determination of p. The value of this parameter would allow verification of the different models for the growth-induced magnetic anisotropy of these films.

The value of p influences the magnitude of the structure factor of the Y^{3+} sublattice, which also depends on the concentration of Bi^{3+} ions. The corresponding calculation (for the fixed value of $x = 0.37$ of the sample studied) shows that if p is changed from 0 to 1 the magnitude of S_h^Y changes from 0.24 to 0.52. It is clear that the value of p also influences the X-ray reflectivity of the layer: for $p = 0$ when all Bi^{3+} ions are on c_{xy} sites and diffract X-rays in phase with the other ions in the lattice, because of the high value of the atomic scattering factor of Bi^{3+} compared to Y^{3+} ions, the reflectivity of the film is maximal.

Thus, it is seen from analysing the position of the Bi^{3+} ions by the XSW method that these ions cannot be considered as impurities which are independent from the other ions in the lattice and their fluorescence yield curve cannot be described by the coherent fraction and coherent position values usually interpreted in XSW experimental results. Therefore, comparing the experimental and theoretical curves it is necessary to take into account the effect the position of the ions has on the scattering characteristics of the other sublattices and on the film lattice as a whole.

In order to calculate the fluorescence yield curves and reflectivity we used a computer program based on an algorithm first suggested by Kovalchuk, Kohn & Lobanovich (1985) (see also Kovalchuk & Kohn, 1986). The program calculates the angular dependencies of the transmission coefficient P_T and reflection coefficient P_R and of the yield of secondary radiation with an exponential function of the yield probability $P(z) = \exp(-z/L_{yi})$ for a multilayer crystal system with sharp boundaries. It is assumed that each layer is represented by a perfect (on average) crystal which can be characterized by constants within the layer thickness: $\Delta d/d$ is the change of the plane spacing, $\exp(-W)$ is the decrease of the coherent-scattering amplitude, and $\chi_{o,h}$ are the Fourier components of the polarizability of the crystal.

Within each layer calculations of the reflection and transmission coefficients and of the yield of secondary radiation are performed analytically. The interaction between layers is taken into account by means of the recurrent relationships which bind the amplitudes of waves on different layer boundaries together. The program also calculates the convolution with the monochromator crystal reflectivity curve taking into account real experimental conditions (asymmetry of the sample and monochromator crystal *etc.*).

In the present paper we consider the model of a two-layer crystal consisting of the thin film and the substrate. The calculated angular curves of the reflectivity and Bi^{3+}-ion fluorescence yield for values of p in the interval 0 to 1 are shown in Figs. 2(*a*) and 2(*b*). The curves were calculated for the real angular range of X-ray diffraction from the crystal lattice of the epitaxial film.

As follows from Fig. 2(*a*), the change of distribution of Bi^{3+} ions indeed leads to a change in the reflectivity of the film though the sensitivity of the X-ray curves to the value of p is rather poor – when p increases from 0 to 1 the maximum reflectivity decreases from 0.53 to 0.39.

The angular yield curves of the Bi^{3+} fluorescence demonstrate, as expected, a strong dependence on the distribution of these ions (Fig. 2*b*). For values $p = 0$ (all Bi^{3+} ions in c_{xy} sites) and $p = 1$ (all Bi^{3+} ions in c_z sites) the amplitude of the structure factor of the Bi^{3+} ions attains its maximum ($|S_h^{Bi}| = 1$) and the phase φ^{Bi} of the structure factor equals 0 and π, respectively. The angular yield curves for these limiting cases show reversed positions for maxima and minima of the yield. When $|S_h^{Bi}|$ decreases the ratio of the fluorescence yield to the background becomes smaller. Note that on the curve corresponding to $p = 0.33$ (uniform distribution of Bi^{3+} ions over c_{xy} and c_z sites) a clear maximum occurs at the high-angle

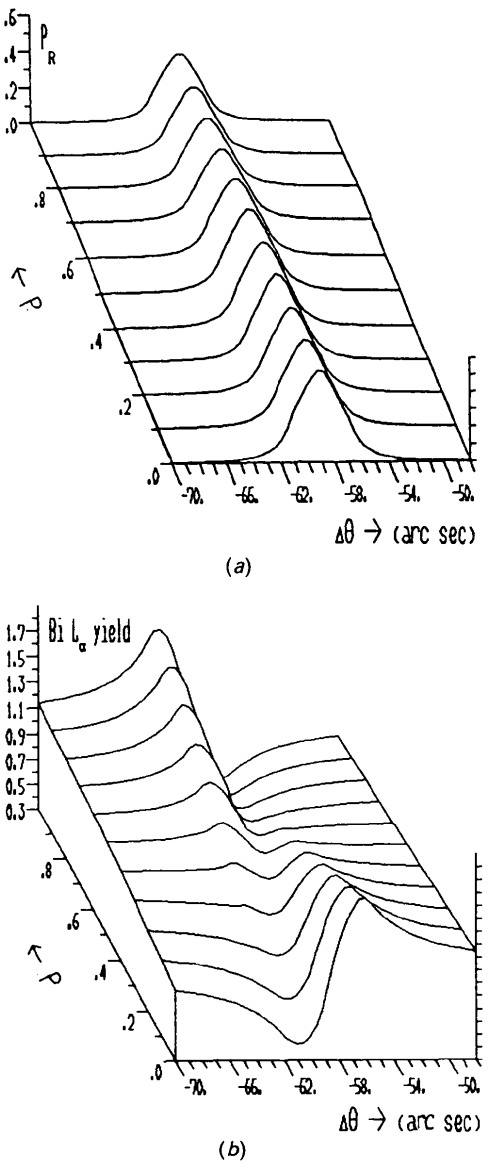

Fig. 2. Calculated angular curves of the reflectivity P_r (*a*) and the angular yield curves of the Bi^{3+} fluorescence (*b*) for values of p from 0 to 1 in the angular range of the X-ray diffraction on the film.

side (with respect to the maximum of Bragg diffraction on the film).

The problem of determination of the distribution of Bi^{3+} ions over dodecahedral sites thus requires the calculation of X-ray reflectivity and fluorescence yield curves for different values of p and their comparison with experimental curves. The effect of p on the structure factors of individual sublattices, as well as on the structure factors of the lattice as a whole must be taken into account. Though the angular yield curve of Bi^{3+} fluorescence is the most sensitive to p value, correspondence between theory and other experimental curves (X-ray reflectivity and angular yield curves of the fluorescence from other ions) may serve as additional confirmation of the correctness of the solution.

4. Experiment

Garnet films were grown by the isothermal dipping LPE method from PbO–B_2O_3 based melts. The films were grown on (001)-oriented substrates of gadolinium gallium garnet at a constant rotation rate of 100 to 150 rev min^{-1}. The selected growth rate was between 0.2 and 1.0 $\mu m\ min^{-1}$, the undercooling 5–70 K and the growth temperature in the range 1053–1253 K (Nevriva, Novak & Cermak, 1985). The film thickness was controlled by the growth time and varied from 2 to 5 μm.

The samples were characterized using X-ray double-crystal topography and diffractometry in the parallel setting with Cu $K\alpha$ radiation. A sufficiently homogeneous and perfect area of one sample ($5 \times 5\ mm^2$) was chosen for the experiment described in the present paper. No satellites of the main-layer maximum were observed with a layer thickness of 3 μm.

The Bi content, $x = 0.37 \pm 0.04$, of the $Y_{3-x}Bi_xFe_5O_{12}$ layer under study was determined by a JEOL LXA 733 X-ray microanalyser using the Bi $M\beta$ line (Kozumplikova, Kub & Simsova, 1983).

Measurements, by the XSW method, were carried out using the double-crystal arrangment (see inset in Fig. 3). We used Mo $K\alpha$ radiation from a conventional X-ray tube with sufficient energy to produce fluorescence excitation from all ions in the sample. A perfect silicon crystal with a symmetrical (111) reflection was used as collimator crystal. The Si(111) reflection was chosen because of the good match of its interplaner spacing ($d_{111} = 3.135$ Å) with the interplanar spacing of the (004) planes of the gadolinium gallium garnet crystal ($d_{400} = 3.096$ Å), giving a negligible value of angular dispersion ($\delta =$ 0.1 arc sec). The (004) reflection of the sample was slightly asymmetrical: the angle ψ between the reflection planes and the surface was $\psi = 2.3°$ which corresponds to an asymmetry factor $\beta = [\sin(\theta_B - \psi)/\sin(\theta_B + \psi)]^{1/2} = 1.5$.

An Si(Li) detector with an energy resolution of 300 eV was used for measurement of the fluorescence radiation. The energy spectrum is shown in Fig. 3. During the experiment the yields within different energy intervals were measured for each point on the rocking curve. The Bi $L\beta$ line was used for registration of the fluorescence from the Bi^{3+} ions. The Y $K\alpha$ line and the background between Bi $L\alpha$ and Bi $L\beta$ lines were measured simultaneously. In addition, a two-dimensional array (angle–energy) was accumulated during the measurement which contained the energy interval lines of Gd $L\alpha$, Fe $K\alpha$, Gd $L\beta$ and Fe $L\beta$ for each angular point. On completion of the experiment a computer analysis was carried out which allowed separation of the contributions from individual lines.

Because of the low-intensity yield of the fluorescence from the bismuth ions ($\simeq 0.3$ Hz), the Bragg reflection region of the film was scanned many times in order to accumulate data. We used a torsion goniometer, piezoelectric driver and electronic feedback system [similar to the one proposed by Krolzig, Materlik & Zegenhagen (1983)]. The electronic system corrects the angular position after each scan and ensures that the center of gravity of the diffraction curve coincides with the center of the angular range scanned during the long time required for the measurement. The total time needed for the measurement was more than 300 h. This time was necessary because of the weak differences between the angular dependence of Bi^{3+} fluorescence and the background (the total number of counts for each point was about 8×10^3). The resulting angular dependencies of the fluorescence yield were normalized to the yield of the off Bragg measurement.

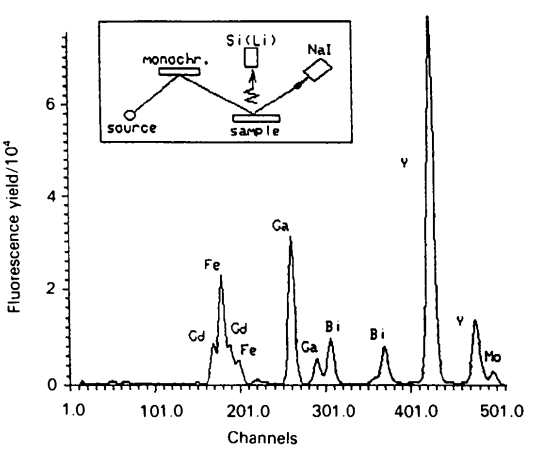

Fig. 3. Energy spectrum of the secondary radiation of the sample, measured with an Si(Li) detector. The experimental arrangement is shown in the inset.

5. Results and discussion

The diffraction curve for the sample studied is shown in Fig. 4. The curve has two diffraction peaks. The left peak, which is the more intense, corresponds to the reflection from the film, while the right peak is the reflection from the substrate. The low intensity of this peak is caused by strong absorption of the radiation which is transmitted through the film twice without diffraction. The angular distance between the two peaks allows a direct determination of the lattice mismatch between the film and substrate $\Delta d/d = 2.5 \times 10^{-3}$. In Fig. 5 the experimental angular dependencies of the fluorescence of Bi^{3+} (5*a*), Y^{3+}(5*b*), Fe^{3+} (5*c*) and Gd^{3+} (5*d*) are shown together with the reflection curve (5*e*) in the angular range corresponding to the diffraction on the film.

As mentioned in §3, the interference structure of the angular dependence of the Bi^{3+} fluorescence yield is relatively weak. In spite of this, two weak maxima may be clearly seen on the experimental curve (Fig. 5*a*). This curve shape may seem rather strange as it shows a very weak difference between the intensity and the background in the angular range where the intensity of the reflected beam is sufficiently large.

This may be understood on the basis of the theory of the XSW method (Kovalchuk & Kohn, 1986) if we consider three factors which influence the shape of the fluorescence yield curve, namely the modulus and the phase of the structure factor of the sublattice of the ions under study, and the extinction effect with the finite thickness of the film taken into account. The experimentally observed shape of the curve is determined by the fact that the Bi^{3+} sublattice structure factor is close to zero and the extinction effect for a given thickness of film leads to the decrease which almost fully compensates the increase of the yield associated with the reflected beam.

This interpretation of the experimental curve is confirmed by Fig. 2(*b*). It is seen that for small and large values of p the curve has a clear interference structure while for $p \simeq 0.5$ the modulus of the structure factor is equal to zero and the calculated curve is close to the experimental one.

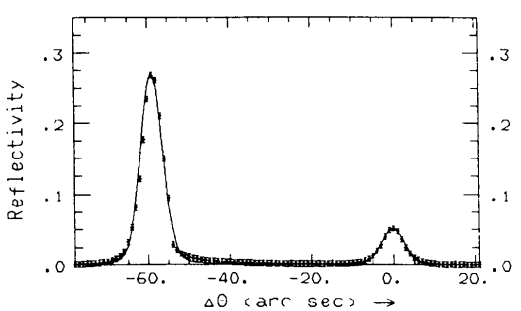

Fig. 4. Experimental and calculated diffraction curves in the angular range of the X-ray diffraction on the film and on the substrate.

The best agreement between experiment and calculation is obtained for p between 0.4 and 0.5. In the final fit p was determined simultaneously with the other parameters which influence the X-ray diffraction and fluorescence yield curves such as the static Debye–Waller factors of the film and the substrate and film thickness. The angular yield curve of Bi^{3+} fluorescence and the X-ray diffraction curve were considered over the whole angular range (Fig. 4). When the convolution with reflectivity curve of the collimator crystal was calculated, the difference in angular widths of both crystals was taken into account. The possibility of a (small) mosaic structure of the sample and angular dispersion were taken into account by additional convolution using the Gaussian function $(1/\sqrt{2\pi\sigma})\exp[-(\Delta\theta)^2/2\sigma^2]$. The best fit was obtained for $p = 0.44 \pm 0.02$, $t = 3$ μm (this value corresponds to an independent measurement), with Debye–Waller factors $\exp(-W_f) = \exp(-W_s) = 0.93$ and $\sigma = 3.8$ arc sec (for comparison, the intrinsic widths of the reflectivity curves of the sample and the monochromator were 3.5 and 3.0 arc sec respectively). The final result, $p = 0.44 \pm 0.02$, was obtained by the least-squares method using only p as a fitting parameter in the range 0.4–0.5 with other parameters fixed. The calculated curves are shown in Figs. 4 and 5(*a*). It is seen that the overall agreement of theory with experiment is satisfactory.

Note that the value $p = 0.44 \pm 0.02$ represents the main result of this work. In principal it is possible to determine the value of p from the diffraction experiment only, since the X-ray diffraction curve also depends on p (see Fig. 2). The accuracy of this approach would be very low, however. The XSW method on the other hand determines the value $p = 0.44$ with satisfactory accuracy. This may be seen from Fig. 5(*a*) where the curve corresponding to $p = 0.33$ is also shown for comparison. However, the diffraction curves calculated for $p = 0.44$ and 0.33 are practically indistinguishable. The angular yield curves of the fluorescence of Y^{3+} and Fe^{3+} ions are shown in Figs. 5(*b*) and 5(*c*). Theoretical curves were calculated with the parameter values given above. The good agreement between experiment and theory is additional confirmation of the correctness of our approach and of the value of p.

Fig. 5(*d*) shows theoretical and experimental angular yield curves of Gd^{3+} fluorescence from the substrate. In spite of the fact that in the angular range of the film diffraction there is practically no diffraction from the substrate, the angular curves have the form of an asymmetrical dip. Note that in this case the

curve of the fluorescence yield is identical to the curve of the transmission coefficient of the film. It is interesting that this is probably the only possible way to measure the transmission coefficient of these films. The usual X-ray diffraction method is useless because of strong absorption in the substrate.

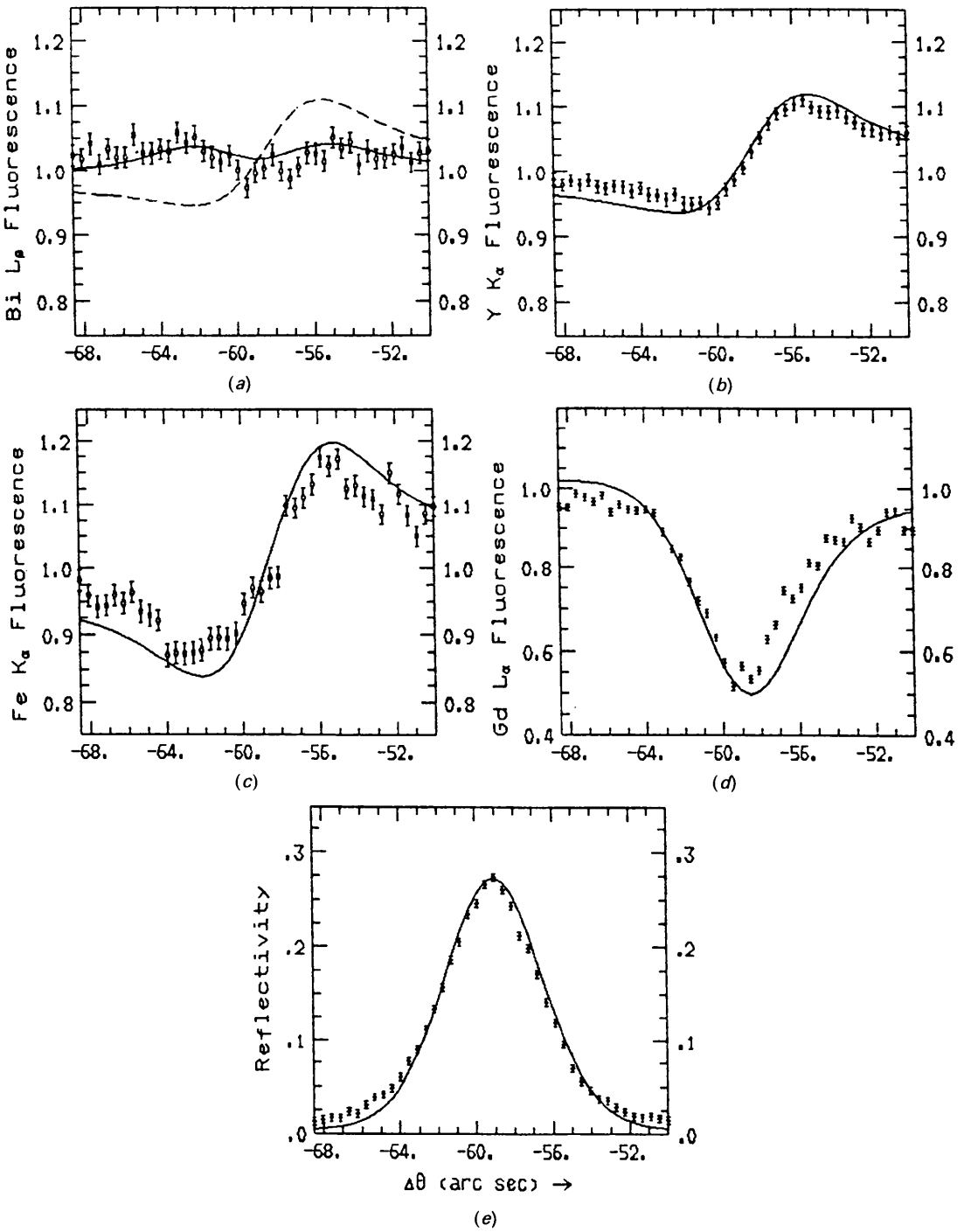

Fig. 5. Experimental and calculated (for $p = 0.44$) angular curves of the fluorescence yield of Bi^{3+} (*a*), Y^{3+} (*b*), Fe^{3+} (*c*) ions from the film and Gd^{3+} ions from the substrate (*d*) and the X-ray diffraction curve (*e*). For comparison the fluorescence yield curve for $p = 0.33$ (uniform distribution of Bi^{3+} ions over c_z and c_{xy} sites) is also shown in (*a*).

6. Concluding remarks

In the present paper we have shown that the problem of preferential distribution of Bi^{3+} ions in the [001]-oriented film of $Y_{3-x}Bi_xFe_5O_{12}$ garnet can be solved in a straightforward way using the XSW method. The same method may also be used for other orientations. We note, however, that in the case of the [111] growth direction the reflections with reciprocal-lattice vectors perpendicular to the surface cannot be used. This is related to the garnet crystallography: for [111]-oriented films different groups of the *c* sites lie in the same planes parallel to the surface and thus cannot be distinguished by the XSW method. In this case an inclined geometry is needed.

The XSW method may also be used to determine the preferential distribution of other kinds of ions, in particular the distribution of rare-earth and yttrium ions over dodecahedral sites may be determined. Finally, we note that if synchrotron radiation, rather than conventional X-ray tubes, were to be used the XSW method could provide a fast and efficient way for the determination of all kinds of preferential distributions of ions in garnet films.

References

BATTERMAN, B. W. (1964). *Phys. Rev. A*, **133**, 759–764.

BATTERMAN, B. W. (1969). *Phys. Rev. Lett.* **22**, 703–705.

BATTERMAN, B. W. & COLE, H. (1964). *Rev. Mod. Phys.* **36**, 681–717.

HANSEN, P. & KRUMME, J. P. (1984). *Thin Solid Films*, **144**, 69–107.

KAZIMIROV, A. YU., KOVALCHUK, M. V. & KOHN, V. G. (1988). *Sov. Tech. Phys. Lett.* **14**(8), 587–588.

KOVALCHUK, M. V. & KOHN, V. G. (1986). *Sov. Phys. Usp.* **29**, 426–446.

KOVALCHUK, M. V., KOHN, V. G. & LOBANOVICH, E. F. (1985). *Sov. Phys. Solid State*, **27**, 2034–2038.

KOZUMPLIKOVA, M., KUB, J. & SIMSOVA, J. (1983). *Proc. Third Course of Advanced Studies in EMA and REM*, pp. 174–178. Poljanka, Czechoslovakia.

KROLZIG, A., MATERLIK, G. & ZEGENHAGEN, J. (1983). *Nucl. Instrum. Methods*, **208**, 613–619.

LAGOMARSINO, S., SCARINCI, F. & TUCCIARONE, A. (1984). *Phys. Rev. B*, **29**, 4859–4863.

NEVRIVA, M., NOVAK, P. & CERMAK, J. (1985). *J. Cryst. Growth*, **71**, 409–418.

NOVAK, P. (1984). *Czech. J. Phys.* **B34**, 1060–1074.

PINSKER, Z. G. (1978). *Dynamical Scattering of X-rays in Crystals*. Berlin: Springer-Verlag.

WINKLER, G. (1981). *Magnetic Garnets*. Braunschweig: Vieweg.

ZHELUDEVA, S. I., ZAKHAROV, B. G., KOVALCHUK, M. V., KOHN, V. G., SOZONTOV, E. A. & SOSFENOV, A. N. (1988). *Sov. Phys. Crystallogr.* **33**(6), 804–807.

Acta Cryst. (1992). **B48**, 584–590

High-Temperature Neutron Powder Diffraction Study of $ZrSiO_4$ up to 1900 K

BY Z. MURSIC

Institut für Kristallographie der Universität, Theresienstrasse 41, 8000 *München* 2, *Germany, and Institut Laue–Langevin, BP* 156 *X*, 38042 *Grenoble CEDEX, France*

T. VOGT

Institut Laue–Langevin, BP 156 *X*, 38042 *Grenoble CEDEX, France*

AND F. FREY

Institut für Kristallographie der Universität, Theresienstrasse 41, 8000 *München* 2, *Germany*

(*Received* 3 *October* 1991; *accepted* 6 *March* 1992)

Abstract

We report here a high-temperature study of synthetic zircon up to 1900 K using high-resolution neutron powder diffraction in combination with a mirror furnace. Zircon ($ZrSiO_4$) is tetragonal, space group $I4_1/amd$, $Z = 4$, $a = 6.605$, $c = 5.987$ Å (room-temperature values). A previously unknown displacive structural change in the vicinity of 1100 K was detected. This 'transition' occurs in the temperature region where metamict zircon crystals recrystalize. Structural changes point towards the tilting of silicate tetrahedra as the driving force for this process. It is useful to describe the Zr—O polyhedral environment as two interpenetrating tetrahedra with a different temperature evolution rather than as a dodecadeltahedron. We have also followed the decomposition of $ZrSiO_4$ into tetragonal ZrO_2 and SiO_2 with the β-cristobalite structure. There is experimental evidence for the gradual disordering of the Zr—O subunit.

Introduction

Zirconium orthosilicate ($ZrSiO_4$) is dimorphous. Besides the dimorph characterized in the *Abstract*,

0108-7681/92/050584-07$06.00